

Strouhal numbers of unsteady flow structures around a simplified car model

Zhang B F¹, Zhou Y¹, To S²

¹Department of Mechanical Engineering, The Hong Kong Polytechnic University,
Hung Hom, Kowloon, Hong Kong SAR, China

²State Key Laboratory in Ultra-precision Machining Technology,
Department of Industrial and System Engineering, The Hong Kong Polytechnic University,
Hung Hom, Kowloon, Hong Kong SAR, China.

INTRODUCTION

There has been recently a renewed interest in finding new technologies to reduce aerodynamic drag and hence fuel consumption in automotive industry because of the lasting high fuel costs in the past few years as well as the issue of global warming. Active control has been identified to be the most likely technique that may achieve substantial drag reduction further. The Ahmed body is perhaps the most widely used simplified vehicle model in the active drag reduction research [1-2]. One piece of the crucial information required for the active control of drag is the Strouhal number $St_{\sqrt{A}}$, based on the square root of the frontal area A , of unsteady flow structure around the Ahmed model. Previously reported $St_{\sqrt{A}}$ is rather scattered, 0.23 ~ 0.31 over the rear window of $\phi = 25^\circ$ and 0.36 ~ 0.49 behind the base. This work aims to clarify this issue and conduct a relatively thorough investigation on $St_{\sqrt{A}}$ in the wake of the Ahmed model based on extensive hotwire and flow visualization measurements.

RESULTS AND DISCUSSION

Experiments were conducted in a closed circuit wind tunnel (fig 1). The 1/3 scaled Ahmed body was placed on a raised floor, which is used to control the boundary layer thickness. The Reynolds number $Re_{\sqrt{A}} (\equiv U_\infty \sqrt{A} / \nu)$, where U_∞ and ν are the free-stream flow velocity and kinematic viscosity, respectively) was 6.59×10^4 . The measured predominated $St_{\sqrt{A}}$ and unsteady instantaneous flow structure above the roof, over the slant and behind the base of Ahmed body are discussed below respectively.

Figure 2 shows the power spectral density function E_u of the single hotwire signal u measured above the roof of the model at two stations downstream of the leading edge. The pronounced peak occurs at $St_{\sqrt{A}} = 0.196$ and 0.140 in figure 2a, depending on the spanwise location. Based on Spohn & Gillieron's [4] flow visualization, the peak $St_{\sqrt{A}} = 0.196$ at $y^* = 0$ and 0.140 at $y^* = 0.14$ are ascribed to the vortices shed from the recirculation bubble at the leading edge and the oscillation of the core of the longitudinal vortices resulting from the bubble pulsation, respectively. Asterisk denotes normalization by \sqrt{A} in this paper. At $y^* = 0.29 \sim 0.36$, the peak at $St_{\sqrt{A}} = 0.196$ is evident. The pronounced peak appears broadened at $y^* = 0.43$ under influence of the shear layer over the side surface. Further downstream, the peak at $St_{\sqrt{A}} = 0.140$ does not seem to be discernible in E_u (Fig. 2b), due to the weakened longitudinal vortex cores as advected downstream.

Figure 3a presents E_u measured at A₁-A₄ in the symmetry plane ($y^*=0$) along the slant surface. The peak at $St_{\sqrt{A}} = 0.196$ is evident at A₁ and A₂, but becomes weaker further downstream at A₃ and vanishes at A₄. The observation is consistent with the previous report [2] of $St_{\sqrt{A}} = 0.22$ measured near this location. The same pronounced peak at $St_{\sqrt{A}} = 0.196$ is observed at B₁-B₄ for $y^* = 0.36$ (Fig. 3b). However, the most pronounced peak occurs at $St_{\sqrt{A}} = 0.265$ near the side edge of the rear window (Fig.3c), which is apparently linked to the C-pillar vortex. Its second harmonic frequency $St_{\sqrt{A}} = 0.530$ is discernible.

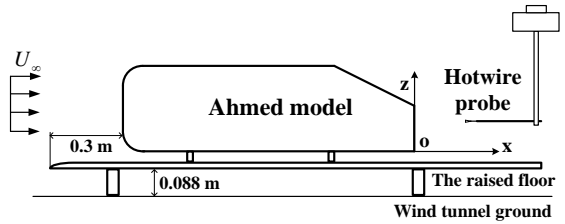


Figure 1 Experimental arrangement

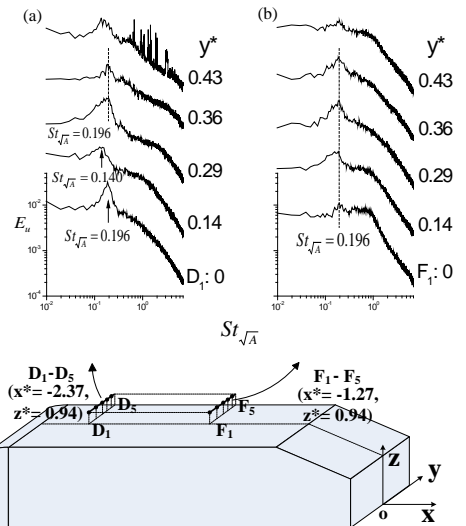


Figure 2 Power spectral density function E_u of hot-wire signals: (a) D₁-D₅; and (b) F₁-F₅.

Figure 4 presents typical photographs captured from flow visualization in the planes of $y^* = 0$ and $y^* = 0.36$ over the rear window. Vortex merging is discernible at $y^* = 0$, as marked in figure 4a, which may be responsible for the disappearance of the peak at A_4 (figure 3a). Flow visualized in the y - z plane at $x^* = -0.34$ shows two pairs of counter-rotating streamwise vortices (not shown), reconfirming Wang et al.'s proposition [4] that the wavy spanwise roll vortices are formed over the slant surface. This spanwise vortex is probably responsible for the peak at $St_{\sqrt{A}} = 0.196$ in E_u over the slant.

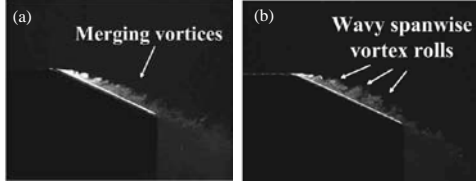


Figure 4 Typical photographs of the flow structure from flow visualization over the slant: (a) $y^* = 0$; (b) $y^* = 0.36$.

Behind the vertical base, a predominant peak is observed in E_u at $St_{\sqrt{A}} = 0.442$ for various downstream stations in the plane of $y^* = 0$ (Fig.5). This peak is only discernible near the ground, i.e., at $K_1 - K_3$, at $x^* = 0.2$. But it grows considerably stronger and evident further away from the ground as x^* increases up to 0.77, and then is weakened for larger x^* . Typical flow structures behind the vertical base (Fig 6), captured from flow visualization, suggest that coherent structures are alternatively emanated from the upper and lower recirculation bubbles, which are responsible for the pronounced peak at $St_{\sqrt{A}} = 0.442$ in E_u (Fig.5). This finding conforms to Vino et al.'s observation [1] that the recirculation bubbles were stretched in the measured turbulence intensity.

CONCLUSIONS

The work leads to following conclusions:

- 1) A quasi-periodical structure of $St_{\sqrt{A}} = 0.140$ is observed above the roof near the leading edge, which is ascribed to the pulsation of the separation bubble from the leading edge.
- 2) Another predominant frequency of $St_{\sqrt{A}} = 0.196$ is measured above the roof, due to the vortices shed from the recirculation bubble at the front. This peak is also detected over the rear window, suggesting that spanwise vortices over the slant are connected to those formed over the roof.
- 3) A strong peak occurs at $St_{\sqrt{A}} = 0.265$ along the side edge of rear window, which is associated with the C-pillar vortex.
- 4) Other than the well reported C-pillar vortices, the wake behind the vertical base is predominated by the quasi-periodical structures of $St_{\sqrt{A}} = 0.442$, which are generated by alternate emanations of coherent structures from upper and lower recirculation bubbles, respectively. These distinct vortices of different $St_{\sqrt{A}}$ explain, at least partially, the rather scattered $St_{\sqrt{A}}$ in the literature.

Acknowledgments

YZ wishes to acknowledge support given to him from Research Grants Council of HKSAR through grant PolyU 5319/12E.

REFERENCES

- [1] Vino G., Watkins S., Mousley P., Watmuff J. & Prasad S. (2005) *Journal of Fluids and Structures* **20**, 673-695.
- [2] Thacker A., Aubrun S., Leroy A. & Devinant P. (2010) AIAA paper 2010-4569.
- [3] Wang X.W., Zhou Y. & Pin Y.F. (2011) *Journal of Fluid Mechanics* (submitted)
- [4] Spohn A. & Gillieron P. In *IUTAM symposium: unsteady separated flows*, Toulouse, France, 2002

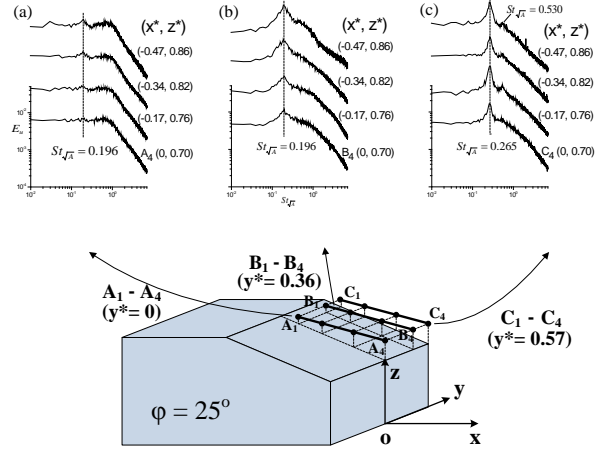


Figure 3 Power spectral density function E_u of hot-wire signals measured along A_1 - A_4 , B_1 - B_4 , C_1 - C_4 , respectively, over the slant.

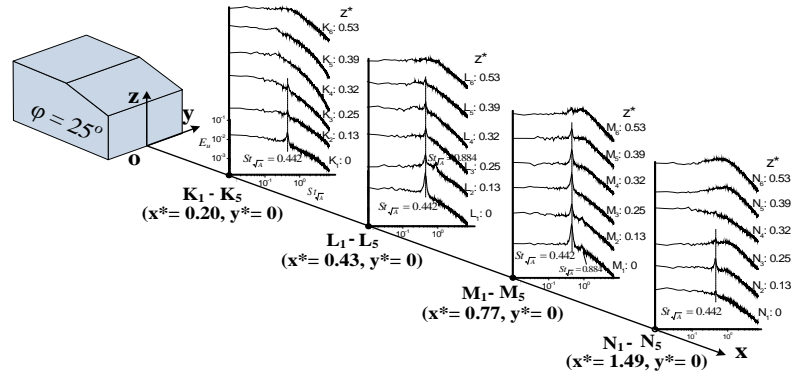


Figure 5 Power spectra E_u of hot-wire signals measured at K_1 - K_6 , L_1 - L_6 , M_1 - M_6 , N_1 - N_6 , respectively, at $y^*=0$ in behind the base.

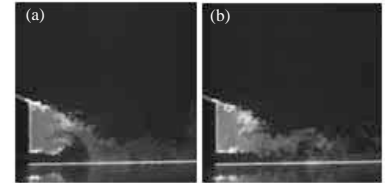


Figure 6 Typical photographs of the flow structure from flow visualization in the symmetry plane: (a) vortex shedding from the upper edge of the base, (b) from the lower edge.